Signal Processing 93 (2013) 3202–3208

Contents lists available at SciVerse ScienceDirect

Signal Processing

journal homepage: www.elsevier.com/locate/sigpro

Transmitter precoder design to improve the performance of the MUSIC algorithm

Li Zhang [a,*], Yong Huat Chew [b], Wai-Choong Wong [c]

[a] NUS Graduate School for Integrative Sciences and Engineering, National University of Singapore, Singapore
[b] Institute for Infocomm Research, Agency for Science, Technology and Research, Singapore
[c] Department of Electrical and Computer Engineering, National University of Singapore, Singapore

ARTICLE INFO

Article history:
Received 21 November 2012
Received in revised form
23 March 2013
Accepted 23 May 2013
Available online 2 June 2013

Keywords:
Angle-of-arrival estimation
Channel state information
Multipath channel
MUSIC
Performance bound
Precoder

ABSTRACT

Using the MUSIC (MUltiple SIgnal Classification) algorithm to estimate the angle-of-arrival (AoA), we derive a new asymptotic error variance bound when the transmitted signal can be pre-processed. We next propose a precoder design to achieve this bound. However, such an optimal precoder requires channel state information at the transmitter (CSIT) exclusive of the receiver array which cannot be separately estimated practically. A more feasible precoder design, which leverages on the feedback CSIT estimated at the receiver, is next proposed. Using the performance of the optimal precoder which achieves the bound asymptotically as a benchmark, the practical precoder design performs close to the optimal precoder even in the high-resolution scenario. Both precoder schemes exhibit performance improvement compared with the case when no precoder is used.

1. Introduction

Accurate AoA estimation has received a significant amount of attention over the last few decades. It is a fundamental problem in many engineering applications, including wireless communications, radar, radio astronomy, sonar, navigation and tracking of objects. Various high resolution algorithms have been proposed, among which the subspace based algorithms [19,9] have drawn much attention due to their low computational complexity and high resolution property in performing AoA estimation. The MUSIC [15] algorithm is a representative subspace based algorithm. There has been considerable research work in either analyzing its performance [10,16–18,3,4] or developing more advanced robust MUSIC algorithms [1,13,5]. In a multipath environment, the MUSIC algorithm can be used to estimate the AoAs of signals impinging on the receive antenna array simultaneously [8]. However, all the efforts to improve the estimation accuracy focus only on the processing of the received signal. It is therefore natural to raise a question: is it possible to improve the estimation accuracy by pre-processing the transmitted signal at the transmitter? In this paper, we aim to improve the performance bound of the MUSIC algorithm through transmit signal design.

The multiple-input multiple-output (MIMO) technology has enabled a significant increase in data transmission rate as well as improving link reliability. The performance can be further enhanced if a precoder is used to exploit the available CSIT before transmission. It essentially functions as a multimode beamformer, optimally matching the input signal on one side to the channel on the other side [22]. In [2], perfect CSIT is used to compute the achievable channel capacity. The authors in [14] have developed a paradigm for optimal designs of precoder and decoder with the objective of minimizing the symbol minimum mean square error (MMSE). In the scenarios where instantaneous CSIT cannot be tracked reliably, CSIT is usually

* Corresponding author. Tel.: +65 97615016.
E-mail addresses: g0901835@nus.edu.sg, zhangli835@gmail.com (L. Zhang), chewyh@i2r.a-star.edu.sg (Y.H. Chew), wong_lawrence@nus.edu.sg (W.-C. Wong).

0165-1684/$ - see front matter
http://dx.doi.org/10.1016/j.sigpro.2013.05.019

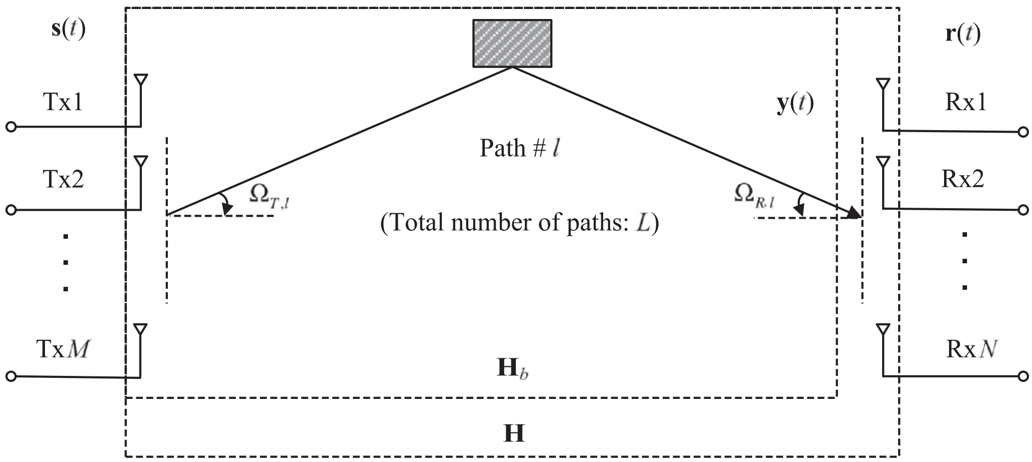

Fig. 1. The flat-fading channel model.

provided in terms of the channel statistics such as channel mean and covariance matrices [21,6,20,7,23].

Although the use of the precoder in the reported work is to increase the achievable system capacity in MIMO communication systems, we apply it to improve the parameter estimation accuracy for position location systems in this paper. Specially we investigate the asymptotic error variance bound in AoA estimation based on the MUSIC algorithm where transmit signal design is possible. The contributions mainly involve two aspects:

- First, when the transmitted signal can be processed before transmission, the performance bound of AoA estimation is derived by minimizing the asymptotic error variance in [17]. We assume a uniform linear array (ULA) at the receiver since the estimation error variance in [17] is only valid for ULA.
- Second, two precoder design strategies are proposed to approach the bound. The optimal precoder can achieve the bound, but it requires CSIT knowledge without the contribution from the receiver ULA which cannot be practically estimated from the received signal. The practical approach which utilizes the feedback channel estimate is next proposed, and our simulation results show that its performance is close to that of the optimal precoder even in the high-resolution scenario.

The rest of the paper is organized as follows. The improved performance bound, as well as the optimal precoder that achieves the bound, is derived in Section 2. In Section 3, the principle behind the practical precoder design is proposed, and its relevance to the optimal precoder is explained. Section 4 presents the simulations, and the performances of the two precoders are analyzed and compared with the bound. Finally, Section 5 concludes the paper.

We use $(\cdot)^T$, $(\cdot)^H$ and $(\cdot)^\dagger$ to denote the transposition, Hermitian transpose and the Moore–Penrose pseudoinverse of the argument, respectively. $\mathrm{tr}(\cdot)$ is the matrix trace. $(\cdot)_{i,k}$ is the i,k element of a matrix. $\mathrm{E}_x\{\cdot\}$ is the expectation with respect to x. The function $\mathrm{diag}(\cdot)$ constructs a diagonal matrix with entries of the argument along the main diagonal.

2. Improving the performance bound of the MUSIC algorithm through transmit signal design

In this section, we describe improvements to the asymptotic error variance bound through appropriate transmit signal design.

2.1. Channel model

We consider a time-invariant flat-fading channel as shown in Fig. 1. The transmitter and the receiver are equipped with M and N omni-directional antennas, respectively. The total number of paths is L. Each path contains three parameters, namely the angle of departure (AoD) $\Omega_{T,l}$, AoA $\Omega_{R,l}$ and complex gain α_l. Each path can be treated as a reflection from the presence of a target. Using the same assumption made in [15], L should be less than $\min(M,N)$ for the purpose of AoA estimation.

The narrowband array assumption [12] is employed here, i.e. the transmit time of the wavefront across the antenna array is assumed to be much smaller than the reciprocal of the signal bandwidth. With this assumption, the steering vector of an array with N elements is defined as $\mathbf{c}(\Omega)=[c_1(\Omega),\dots,c_N(\Omega)]^T$, where Ω is the direction of the wave. Specifically, for a ULA, it has the following expression:

$$\mathbf{c}(\Omega)=[1,\exp(j\omega),\dots,\exp(j(N-1)\omega)]^T, \tag{1}$$

where $\omega=2\pi d_h\cos\Omega/\lambda_s$, d_h is the distance between two adjacent antennas and λ_s is the wavelength.

For the lth propagation path, the mth transmit antenna gain response due to the AoD $\Omega_{T,l}$ is $c_{T,m}(\Omega_{T,l})$ and the nth receive antenna gain response due to the AoA $\Omega_{R,l}$ is $c_{R,n}(\Omega_{R,l})$. With the transmitted signal denoted by $\mathbf{s}(t)=[s_1(t),\dots,s_M(t)]^T$, the received signal for the nth antenna is expressed as

$$r_n(t)=\sum_{m=1}^{M}\sum_{l=1}^{L}\alpha_l c_{T,m}(\Omega_{T,l})c_{R,n}(\Omega_{R,l})s_m(t)+z_n(t), \tag{2}$$

where $z_n(t)$ is the complex white Gaussian noise with mean of zero and variance σ_z^2.

We define $\mathbf{C}_T(\boldsymbol{\Omega}_T)$ and $\mathbf{C}_R(\boldsymbol{\Omega}_R)$ as the transmit and receive steering matrices with $\mathbf{c}_T(\Omega_{T,l})$ and $\mathbf{c}_R(\Omega_{R,l})$ being the lth column, $l=1,\ldots,L$, respectively. We further denote $\mathbf{H}_\alpha = \mathrm{diag}\{\alpha_1,\ldots,\alpha_L\}$. Thus, the channel model may be expressed in a matrix form as

$$\mathbf{r}(t) = \mathbf{H}\mathbf{s}(t) + \mathbf{z}(t), \tag{3}$$

where

$$\mathbf{H} = \mathbf{C}_R(\mathbf{\Omega}_R)\mathbf{H}_\alpha\mathbf{C}_T^T(\mathbf{\Omega}_T),$$

$$\mathbf{r}(t) = [r_1(t),\ldots,r_N(t)]^T,$$

$$\mathbf{z}(t) = [z_1(t),\ldots,z_N(t)]^T.$$

We also define $\mathbf{H}_b = \mathbf{H}_\alpha\mathbf{C}_T^T(\mathbf{\Omega}_T)$, which is the channel matrix exclusive of the receiver array. The signal impinging on the receive antenna array is $\mathbf{y}(t)$, and is expressed as $\mathbf{y}(t) = \mathbf{H}_b\mathbf{s}(t)$. For convenience, we omit the time index t hereafter.

2.2. Performance bound

We use the sum of the error variances for the L AoA estimates as the metric to evaluate the performance of the MUSIC algorithm. As shown in [17], when the receiver is a ULA and N increases, the sum of the variances approaches the following limit:

$$\begin{aligned}\mathrm{var}_{MU}(\boldsymbol{\omega}_R) &= \sum_{l=1}^{L} \mathrm{E}_{\hat{\omega}_{R,l}}[(\hat{\omega}_{R,l}-\omega_{R,l})^2] \\ &= \frac{6\sigma_z^2}{IN^3}\,\mathrm{tr}(\mathbf{P}^{-1}),\end{aligned} \tag{4}$$

where $\boldsymbol{\omega}_R = [\omega_{R,1},\ldots,\omega_{R,L}]$ is the parameter vector under estimation, with $\omega_{R,l} = 2\pi d_h \cos\Omega_{R,l}/\lambda_s$, $l=1,\ldots,L$, and $\hat{\omega}_{R,l}$ is the estimate of $\omega_{R,l}$. I denotes the number of samples used when performing the estimation. $\mathbf{P} = \mathrm{E}_{\mathbf{y}}[\mathbf{y}\mathbf{y}^H]$ is the covariance matrix of $\mathbf{y}$.

Defining $\mathbf{Q} = \mathrm{E}_{\mathbf{s}}[\mathbf{s}\mathbf{s}^H]$ which is the covariance matrix of the transmitted signal $\mathbf{s}$, we have $\mathbf{P} = \mathbf{H}_b\mathbf{Q}\mathbf{H}_b^H$. The problem can be formulated as minimizing the error variance under the transmit power constraint as follows:

$$\begin{aligned}&\min_{\mathbf{Q}} \quad \mathrm{tr}((\mathbf{H}_b\mathbf{Q}\mathbf{H}_b^H)^{-1}) \\ &\text{subject to } \mathrm{tr}(\mathbf{Q}) = P_w \\ &\quad \mathbf{Q} \succcurlyeq \mathbf{0}\end{aligned} \tag{5}$$

where P_w is the total transmission power, and the second constraint means that $\mathbf{Q}$ should be positive semidefinite. We have ignored the scaling factor in the objective function since it does not affect the final solution. The design problem now becomes how we can obtain the optimal transmit covariance matrix $\mathbf{Q}$.

Theorem 1. *Let the truncated singular value decomposition (SVD) of $\mathbf{H}_b$ be given by $\mathbf{H}_b = \mathbf{U}_b\mathbf{\Lambda}_b\mathbf{V}_b^H$, where $\mathbf{U}_b$ and $\mathbf{V}_b$ are $L\times L$ and $M\times L$ matrices with the property $\mathbf{U}_b^H\mathbf{U}_b = \mathbf{I}$ and $\mathbf{V}_b^H\mathbf{V}_b = \mathbf{I}$, respectively, and $\mathbf{\Lambda}_b$ is a $L\times L$ diagonal matrix with its diagonal elements being the singular values of $\mathbf{H}_b$ permutated in decreasing order. Then the optimal transmit covariance matrix that minimizes the cost function in (5) should take the form $\mathbf{Q} = \mathbf{V}_b\mathbf{\Sigma}_b\mathbf{V}_b^H$, where $\mathbf{\Sigma}_b$ is a diagonal matrix.*

Proof. Substituting the truncated SVD into the cost function in (5), we have

$$\mathrm{tr}((\mathbf{H}_b\mathbf{Q}\mathbf{H}_b^H)^{-1}) = \mathrm{tr}((\mathbf{U}_b\mathbf{\Lambda}_b\mathbf{V}_b^H\mathbf{Q}\mathbf{V}_b\mathbf{\Lambda}_b^H\mathbf{U}_b^H)^{-1}). \tag{6}$$

Since $\mathbf{U}_b$ and $(\mathbf{\Lambda}_b\mathbf{V}_b^H\mathbf{Q}\mathbf{V}_b\mathbf{\Lambda}_b^H)$ are both full rank, (6) can be simplified to

$$\begin{aligned}\mathrm{tr}((\mathbf{U}_b^H)^{-1}(\mathbf{\Lambda}_b\mathbf{V}_b^H\mathbf{Q}\mathbf{V}_b\mathbf{\Lambda}_b^H)^{-1}\mathbf{U}_b^{-1}) &= \mathrm{tr}((\mathbf{\Lambda}_b\mathbf{V}_b^H\mathbf{Q}\mathbf{V}_b\mathbf{\Lambda}_b^H)^{-1}) \\ &= \mathrm{tr}(\mathbf{\Lambda}_b^{-2}\mathbf{\Sigma}_b^{-1}),\end{aligned} \tag{7}$$

where $\mathbf{\Sigma}_b = \mathbf{V}_b^H\mathbf{Q}\mathbf{V}_b$.

Next, we need to prove that $\mathbf{\Sigma}_b$ should be diagonal for (7) to be minimized. We use the following lemma [11].

Lemma 1. *If $\mathbf{U}$ and $\mathbf{V}$ are $n\times n$ positive semidefinite Hermitian matrices with eigenvalues $\lambda_i(\mathbf{U})$ and $\lambda_i(\mathbf{V})$, respectively, arranged in decreasing order, and $\lambda_i(\mathbf{U}\mathbf{V})$ are the eigenvalues of the product matrix $\mathbf{U}\mathbf{V}$, then*

$$\mathrm{tr}(\mathbf{U}\mathbf{V}) = \sum_{i=1}^{n}\lambda_i(\mathbf{U}\mathbf{V}) \ge \sum_{i=1}^{n}\lambda_i(\mathbf{U})\lambda_{n-i+1}(\mathbf{V}). \tag{8}$$

From the proof in [7], we know that if matrix $\mathbf{U}$ in Lemma 1 is diagonal, the equality in (8) holds only when matrix $\mathbf{V}$ is also diagonal, and vice versa. In addition, the arrangement of diagonal elements of the two matrices should be in the reverse order.

Applying Lemma 1 and the above conclusion to (7), the fact that $\mathbf{\Lambda}_b^{-2}$ is diagonal implies that $\mathbf{\Sigma}_b^{-1}$ must be diagonal, so that the equality in (8) holds and (7) obtains its minimum. So $\mathbf{\Sigma}_b$ is also diagonal. Besides, the diagonal elements of $\mathbf{\Sigma}_b^{-1}$ must be arranged in the reverse order with that for $\mathbf{\Lambda}_b^{-2}$. Thus, we have

$$\begin{aligned}&\mathbf{V}_b^H\mathbf{Q}\mathbf{V}_b = \mathbf{\Sigma}_b \\ &\Rightarrow \mathbf{Q} = \mathbf{V}_b\mathbf{\Sigma}_b\mathbf{V}_b^H.\end{aligned} \tag{9}$$

Thus, Theorem 1 is proved. □

By applying Theorem 1, the solution which also fulfills the two constraints given in (5) can be computed as follows.

We denote $\mathbf{\Sigma}_b = \mathrm{diag}\{\sigma_{b,1},\ldots,\sigma_{b,L}\}$ and $\mathbf{\Lambda}_b = \mathrm{diag}\{\lambda_{b,1},\ldots,\lambda_{b,L}\}$, where $\lambda_{b,l}$, $l=1,\ldots,L$, are the nonzero singular values of $\mathbf{H}_b$. Substituting (9) into (6), we have

$$\mathrm{tr}((\mathbf{H}_b\mathbf{Q}\mathbf{H}_b^H)^{-1}) = \sum_{l=1}^{L}\frac{1}{\lambda_{b,l}^2\sigma_{b,l}}. \tag{10}$$

Furthermore, the power constraint is simplified to $\mathrm{tr}(\mathbf{Q}) = \sum_{l=1}^{L}\sigma_{b,l} = P_w$. The simplified objective function may then be expressed as

$$\begin{aligned}&\min_{\sigma_{b,l},\,l=1,\ldots,L} \quad \sum_{l=1}^{L}\frac{1}{\lambda_{b,l}^2\sigma_{b,l}} \\ &\text{subject to } \sum_{l=1}^{L}\sigma_{b,l} = P_w \\ &\sigma_{b,l} \ge 0, \quad l=1,\ldots,L\end{aligned} \tag{11}$$

The Hessian matrix of the cost function in (11) is a diagonal matrix as follows:

$$\mathbf{H}_e = \begin{bmatrix} 2\lambda_{b,1}^{-2}\sigma_{b,1}^{-3} & \cdots & 0 \\ \vdots & \ddots & \vdots \\ 0 & \cdots & 2\lambda_{b,L}^{-2}\sigma_{b,L}^{-3}\end{bmatrix}. \tag{12}$$

So it is positive definite in the solution domain which implies that the objective function (11) is convex.

Applying the Lagrange multiplier method, the cost function is written as

$$f(\lambda, \sigma_{b,1}, \dots, \sigma_{b,L}) = \sum_{l=1}^{L} \frac{1}{\lambda_{b,l}^2 \sigma_{b,l}} + \lambda\left(\sum_{l=l}^{L} \sigma_{b,l} - P_w\right), \tag{13}$$

where $\lambda \ge 0$ is the Lagrange multiplier associated with the power constraint.

The cost function in (13) is minimized when its derivatives over $\sigma_{b,l}$, $l = 1, \dots, L$, are all equal to zero. Thus we have

$$\frac{\partial f}{\partial \sigma_{b,l}} = -\frac{1}{\lambda_{b,l}^2 \sigma_{b,l}^2} + \lambda = 0, \quad l = 1, \dots, L. \tag{14}$$

Solving (14) and then determining λ from the equality $\sum_{l=1}^{L} \sigma_{b,l} = P_w$, we obtain the result as

$$\sigma_{b,l} = \frac{P_w}{\lambda_{b,l} \sum_{j=1}^{L} 1/\lambda_{b,j}}, \quad l = 1, \dots, L. \tag{15}$$

The last step is to verify that the diagonal elements of $\mathbf{\Sigma}_b^{-1}$ are arranged in the inverse order of those of $\mathbf{\Lambda}_b^{-2}$, so that the equality in (8) holds. According to (15), the diagonal elements of $\mathbf{\Sigma}_b^{-1}$ are arranged in decreasing order, while those of $\mathbf{\Lambda}_b^{-2}$ are in increasing order.

We conclude that the optimal transmit covariance matrix $\mathbf{Q}$ can be expressed as

$$\mathbf{Q}_{opt} = \mathbf{V}_b \mathbf{\Sigma}_b \mathbf{V}_b^H, \tag{16}$$

where $\mathbf{\Sigma}_b$ is diagonal with the diagonal elements given by (15).

We finally obtain the lower bound by substituting (16) into (4) as follows:

$$\mathrm{var}_{MU}(\boldsymbol{\omega}_R) = \frac{6\sigma_z^2}{IN^3 P_w}\left(\sum_{l=1}^{L} \frac{1}{\lambda_{b,l}}\right)^2, \tag{17}$$

where $\lambda_{b,l}$, $l = 1, \dots, L$, are the singular values of $\mathbf{H}_b$.

2.3. Optimal precoder

The above performance bound can be achieved when an optimal precoder is adopted. As shown in Fig. 2, the input signal $\mathbf{x}(t)$ to the precoder matrix which is derived from the CSIT is K uncorrelated data streams each allocated with equal power P_w/K. The output of the precoder is $\mathbf{s}(t)$, which is expressed as $\mathbf{s}(t) = \mathbf{F}\mathbf{x}(t)$. With this model, the transmit covariance matrix $\mathbf{Q}$ has the following expression:

$$\mathbf{Q} = \mathrm{E}_{\mathbf{x}}[\mathbf{F}\mathbf{x}\mathbf{x}^H\mathbf{F}^H] = \frac{P_w}{K}\mathbf{F}\mathbf{F}^H. \tag{18}$$

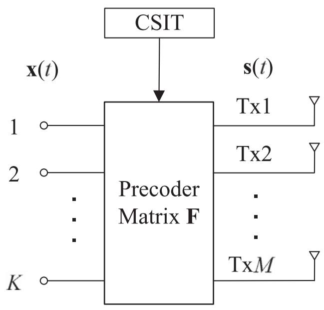

Fig. 2. Precoder model.

The optimal $\mathbf{Q}_{opt}$ has been derived in (16), hence the optimal precoder $\mathbf{F}_{opt}$ can be obtained by taking square root of $(K/P_w)\mathbf{Q}_{opt}$, i.e. $\mathbf{F}_{opt} = \sqrt{(K/P_w)}\mathbf{Q}_{opt}^{1/2}$.

Let us remark that our proposed approach is different from [14, III.A] in terms of motivation, formulation and solutions. Our work is motivated by enhancing the performance of the MUSIC algorithm, and minimizing the asymptotic AoA estimation error is the design criterion. On the other hand, the design objective of the precoder in [14, III.A] is to minimize the minimum mean square error (MMSE) of the received symbol. The two different design criteria lead to two different cost functions, and therefore provide two different optimal precoders.

3. Practical precoder design

The optimal precoder can achieve the performance bound, however, to obtain the matrix $\mathbf{H}_b$ which is required at the transmitter may not be practically possible. Instead, it is more possible to make the receiver estimate the channel matrix $\mathbf{H}$ and introduce a feedback channel from the receiver to the transmitter [22]. In this subsection, we propose a practical precoder design based on the feedback CSIT which will be demonstrated to have the performance close to the optimal precoder later.

We postulate the objective function (5) using the following:

$$\begin{aligned} &\min_{\mathbf{Q}} \ \mathrm{tr}\left(\left(\frac{1}{N}\mathbf{H}\mathbf{Q}\mathbf{H}^H\right)^{\dagger}\right) \\ &\text{subject to } \mathrm{tr}\,(\mathbf{Q}) = P_w \\ &\quad \mathbf{Q} \succcurlyeq \mathbf{0} \end{aligned} \tag{19}$$

and its relevance to the optimal precoder will be demonstrated afterwards. The solution to (19) can be similarly obtained using the method in the previous section. Let the truncated SVD of $\mathbf{H}$ be given by $\mathbf{H} = \mathbf{U}_h \mathbf{\Lambda}_h \mathbf{V}_h^H$, where $\mathbf{U}_h$ and $\mathbf{V}_h$ are $N \times L$ and $M \times L$ matrices with the property $\mathbf{U}_h^H \mathbf{U}_h = \mathbf{I}$ and $\mathbf{V}_h^H \mathbf{V}_h = \mathbf{I}$, respectively, and $\mathbf{\Lambda}_h = \mathrm{diag}\{\lambda_{h,1}, \dots, \lambda_{h,L}\}$ is a $L \times L$ diagonal matrix with its diagonal elements being the singular values of $\mathbf{H}$ permutated in decreasing order. After simplifications, the objective function can be rewritten as $N\,\mathrm{tr}(\mathbf{\Lambda}_h^{-2}\mathbf{\Sigma}_h^{-1})$, where $\mathbf{\Sigma}_h = \mathbf{V}_h^H \mathbf{Q} \mathbf{V}_h$, which is similar to (7). In order to obtain the solution, $\mathbf{\Sigma}_h$ should be a diagonal matrix. Denoting $\mathbf{\Sigma}_h = \mathrm{diag}\{\sigma_{h,1}, \dots, \sigma_{h,L}\}$ and using the Lagrange method, the solution for the transmit covariance matrix when $\mathbf{H}$ is used is given by

$$\begin{cases} \mathbf{Q}_{prac} = \mathbf{V}_h \mathbf{\Sigma}_h \mathbf{V}_h^H \\ \sigma_{h,l} = \frac{P_w}{\lambda_{h,l} \sum_{j=1}^{L} 1/\lambda_{h,j}}, \quad l = 1, \dots, L. \end{cases} \tag{20}$$

From this result, we can see that the diagonal elements of $\mathbf{\Sigma}_h^{-1}$ are arranged in decreasing order, which is opposite to $\mathbf{\Lambda}_h^{-2}$. Similar to the optimal precoder, the practical precoder $\mathbf{F}_{prac}$ can be obtained by taking the square root of $(K/P_w)\mathbf{Q}_{prac}$, i.e. $\mathbf{F}_{prac} = \sqrt{(K/P_w)}\mathbf{Q}_{prac}^{1/2}$.

We shall show the impact on the estimated error variance when $\mathbf{H}$ is used instead of $\mathbf{H}_b$. Since $\mathbf{H} = \mathbf{C}_R(\mathbf{\Omega}_R)\mathbf{H}_b$, by

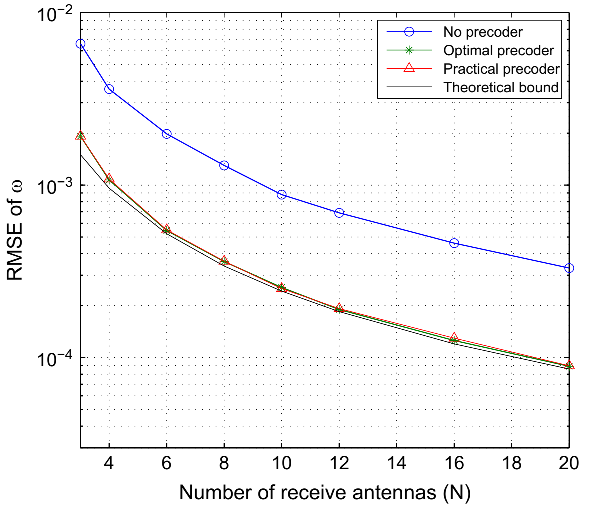

Fig. 3. Comparison of performance bound and the performances of precoders as a function of the number of receive antennas (SNR=20 dB, $\phi=2\theta_{3\ \mathrm{dB}}$).

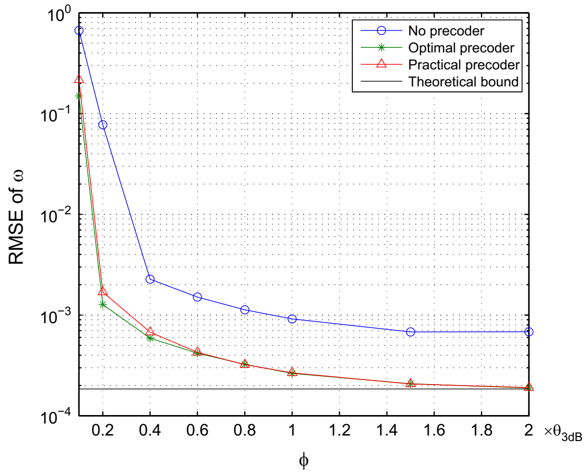

Fig. 4. Comparison of the three AoA estimation strategies as a function of the angle of separation ϕ (N=12, SNR=20 dB).

substituting this into the matrix trace in (19), we have

$$\begin{aligned}
&\mathrm{tr}\left(\left(\frac{1}{N}\mathbf{C}_R(\mathbf{\Omega}_R)\mathbf{H}_b\mathbf{Q}\mathbf{H}_b^H\mathbf{C}_R(\mathbf{\Omega}_R)^H\right)^{\dagger}\right)\\
&\quad=\mathrm{tr}\left(\left(\frac{1}{N}\mathbf{C}_R(\mathbf{\Omega}_R)^H\mathbf{C}_R(\mathbf{\Omega}_R)\right)^{-1}\left(\mathbf{H}_b\mathbf{Q}\mathbf{H}_b^H\right)^{-1}\right)\\
&\quad=\mathrm{tr}(\mathbf{R}_c^{-1}(\mathbf{H}_b\mathbf{Q}\mathbf{H}_b^H)^{-1}),
\end{aligned}\tag{21}$$

where $\mathbf{R}_c=(1/N)\mathbf{C}_R(\mathbf{\Omega}_R)^H\mathbf{C}_R(\mathbf{\Omega}_R)$. For ULA, the steering vector has the form given in (1), so the entries of $\mathbf{R}_c$ can be expressed as

$$(\mathbf{R}_c)_{i,k}=\begin{cases}1, & i=k\\ \dfrac{1}{N}\sum\limits_{n=1}^{N}\exp(-j(n-1)(\omega_{R,i}-\omega_{R,k})), & i\neq k\end{cases}\tag{22}$$

It can be seen that when the AoAs are sufficiently separated, the off-diagonal elements of $\mathbf{R}_c$ are much smaller than the diagonal elements when N is large. Under this condition, $\mathbf{R}_c$ can be approximated to an identity matrix since the off-diagonal elements are small numbers. This explains that the trace obtained in (19) approaches that given in (5) if all AoAs are reasonably separated. Our simulation results will later verify this.

The proposed precoder scheme can be applied to the AoA estimation scenarios where transmit signal pre-processing is possible, such as the MIMO radar. Each path in the channel model of Section 2.1 can be treated as a reflection from a target. The overall performance of estimating the AoAs of multiple targets can be improved through such a processing technique.

4. Simulation and performance analysis

The performance of the proposed algorithm is evaluated in a synthetically generated channel. The channel is assumed to have two propagation paths, and the AoAs of the two paths are separated by an angle ϕ whose value varies in the following simulation. The transmitter and receiver are each equipped with a ULA with antenna elements separated by $d_h=\lambda_s/2$. The number of transmit antennas is six, while the number of receive antennas varies in the simulation. We define $\theta_{3\ \mathrm{dB}}$ as the 3 dB beamwidth of the receiver array whose value is given by $\theta_{3\ \mathrm{dB}}=0.891\lambda_s/(Nd_h)$ when $N\leq 30$ [19]. The input to the precoder consists of two independent pseudo-noise (PN) sequences. At the receiver, the number of samples used for the MUSIC algorithm is 1000. The impact on the receive power due to the channel gain is removed through proper normalization. The signal-to-noise ratio (SNR) is defined as the ratio of the transmission power to the noise power at the receiver. As the channel has been normalized, the SNR below can be treated as transmitter or receiver SNR.

The whole simulation consists of two parts. The first part discusses the conditions under which the precoder strategies approach the theoretical bound given in (17), while the second part studies the performance of the precoders in the high-resolution scenarios, i.e. $\phi\leq 0.5\theta_{3\ \mathrm{dB}}$.

4.1. Asymptotic performance of precoder strategies compared with the theoretical bound

Since the theoretical bound shown in (17) is an asymptotic error variance, this part of the simulation demonstrates the conditions for the precoding strategies to approach the bound. We perform two simulations to study the AoA estimate errors of two precoding strategies and compare them with the bound.

Firstly, the performances are shown when the number of receive antennas N changes. The separation angle ϕ is maintained at $2\theta_{3\ \mathrm{dB}}$, so that the effect of closely separated signals which degrades the performance of the MUSIC algorithm can be eliminated. The AoAs of the two paths are set at 90° and $90^\circ+\phi$, while the corresponding AoDs are set at 130° and 30°, respectively. The amplitudes of the instantaneous complex path gains used before normalization are 0.8 and 0.4. In Fig. 3, the performance curves

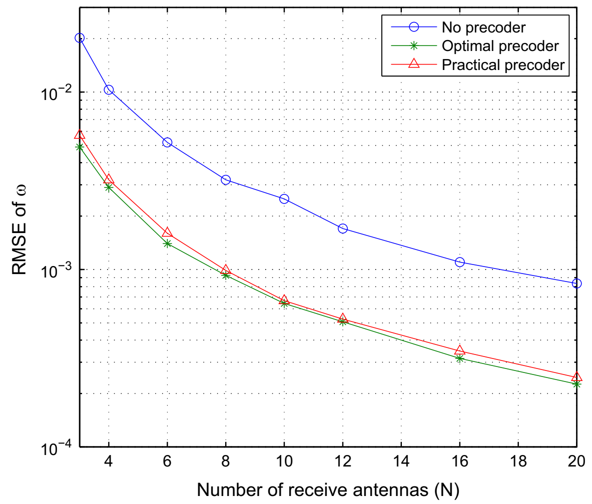

Fig. 5. Performances of precoders as a function of the number of receive antennas in the high-resolution scenario (SNR=20 dB, $\phi=0.5\theta_{3\ \mathrm{dB}}$).

obtained by using the optimal and practical precoders are compared with the achievable performance bound, as a function of N and with SNR set at 20 dB. The RMSE of ω is used as the performance metric, where $\omega=\pi\ \cos\ \Omega$ and Ω is the AoA in degree. We see that the results of precoders get closer to the bound when N increases. When N is sufficiently large, the two curves converge, indicating that the AoA error variances have approached the theoretical limit. In the same figure, the system without precoder is also shown and is found to perform significantly worse.

Secondly, we compare the bound and the two precoder strategies while changing the value of ϕ from $0.1\theta_{3\ \mathrm{dB}}$ to $2\theta_{3\ \mathrm{dB}}$. The SNR is again set at 20 dB. The number of receive antennas is set to be sufficiently large, and in our case we choose $N=12$. From Fig. 4, we can see that as ϕ increases, the two precoder strategies approach the bound asymptotically. Specifically, when $\phi\geq 2\theta_{3\ \mathrm{dB}}$, the MUSIC algorithm with a precoder can achieve the bound. This figure also shows the impact of estimation error when the practical precoder is used instead of optimal precoder. The two precoders get closer when ϕ increases. When $\phi>0.6\theta_{3\ \mathrm{dB}}$, the performance of the practical precoder is already very close to that of the optimal precoder. This observation provides a proof of the correctness of the theoretical explanation in Section 3. On the other hand, when ϕ is small, e.g. $\phi=0.2\theta_{3\ \mathrm{dB}}$, although the performance of practical precoder degrades, it still shows significant improvement over the system without precoder.

4.2. Performance of precoder strategies in the high-resolution scenario

In this part, we demonstrate the performances of the two precoders in the high-resolution scenario (i.e. $\phi\leq 0.5\theta_{3\ \mathrm{dB}}$) which requests the use of the MUSIC algorithm. In our simulation, we choose $\phi=0.5\theta_{3\ \mathrm{dB}}$, and the following two asymptotic schemes are studied.

The first scheme is to increase the number of antennas N while maintaining the SNR at 20 dB. The AoDs and path gains are the same as those in the first part of the simulation. The result is shown in Fig. 5. In such a scenario, the performances of the MUSIC algorithm with and without precoder are degraded compared with Fig. 3. Even though, the estimation with a precoder exhibits significantly better performances than the estimation without precoder. For example, the system with 8 antennas and a practical precoder has nearly the same performance as the one with 20 antennas but without a precoder.

The second scheme studies the performances while increasing the SNR and maintaining $N=12$. The RMSEs of ω are computed and shown in Fig. 6(a) when the SNR changes from −10 dB to 20 dB. Compared with when no precoder is used, the two AoA estimation algorithms with precoders show significant improvement in the performance. To achieve the same RMSE, the improvement is about 10 dB in SNR. The RMSEs of AoA estimation in degrees which is more intuitive in angle estimation is shown in Fig. 6(b).

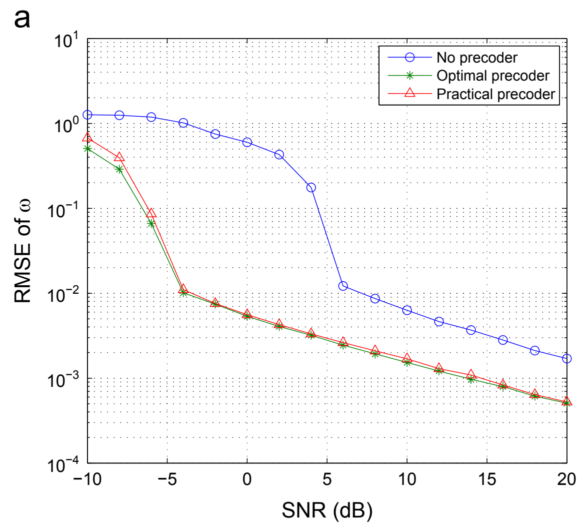

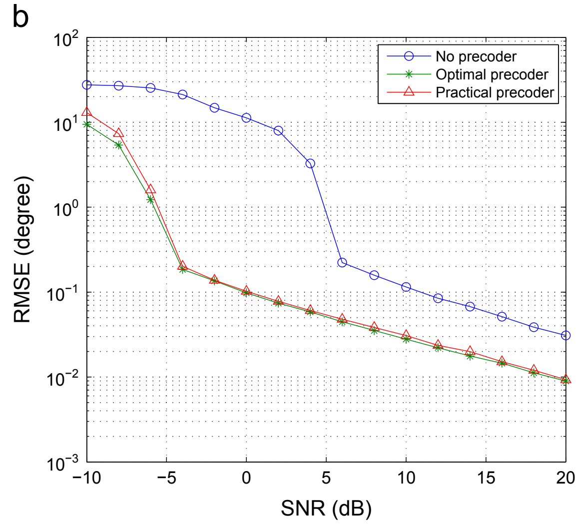

Fig. 6. Comparison of the performances of the three AoA estimation strategies over SNR ($N=12$, $\phi=0.5\theta_{3\ \mathrm{dB}}$): (a) RMSE of ω versus SNR and (b) RMSE of AoAs in degree versus SNR.

5. Conclusion

We have derived a new asymptotic error variance bound when the transmitted signal can be pre-processed while the MUSIC algorithm is used to estimate the AoAs. We further propose the optimal design of a precoder to achieve the bound asymptotically, and a practical precoder design which is realizable in practice. The performance of the optimal precoder is demonstrated to be able to approach the bound asymptotically through simulation. On the other hand, the practical precoder is shown to perform close to the optimal precoder even in the high-resolution scenario. The two precoder schemes can considerably improve performance as compared with the case when no precoder is used, i.e. without any transmit signal design.

Although the proposed precoder schemes can achieve the bound asymptotically, there is still some performance degradation in the high-resolution scenario which makes the performances of the MUSIC algorithm with and without a precoder diverge from the performance limit, as shown in Fig. 4. Thus, there is still room to improve the performance of the algorithm in the high-resolution scenario.

Acknowledgments

This work was partially supported by National Research Funding grant NRF2007IDM-IDM002-069 on Life Spaces (POEM) from the IDM Project Office, Media Development Authority of Singapore. The authors would like to acknowledge the anonymous reviewers for their valuable comments.

References

[1] A. Barabell, Improving the resolution performance of eigenstructure-based direction-finding algorithms, in: Proceedings of the International Conference on Acoustics, Speech, and Signal Processing, vol. 8, pp. 336–339.
[2] T. Cover, J. Thomas, Elements of Information Theory, Wiley-Interscience, New York, 1991.
[3] A. Ferreol, P. Larzabal, M. Viberg, On the asymptotic performance analysis of subspace DOA estimation in the presence of modeling errors: case of MUSIC, IEEE Transactions on Signal Processing 54 (2006) 907–920.
[4] A. Ferreol, P. Larzabal, M. Viberg, On the resolution probability of MUSIC in presence of modeling errors, IEEE Transactions on Signal Processing 56 (2008) 1945–1953.
[5] B. Friedlander, The root-MUSIC algorithm for direction finding with interpolated arrays, Signal Processing 30 (1993) 15–29.
[6] S.A. Jafar, A. Goldsmith, Transmitter optimization and optimality of beamforming for multiple antenna systems, IEEE Transactions on Wireless Communications 3 (2004) 1165–1175.
[7] S.A. Jafar, S. Vishwanath, A. Goldsmith, Channel capacity and beamforming for multiple transmit and receive antennas with covariance feedback, in: Proceedings of the IEEE International Conference on Communications, vol. 7, pp. 2266–2270.
[8] R. Klukas, M. Fattouche, Line-of-sight angle of arrival estimation in the outdoor multipath environment, IEEE Transactions on Vehicular Technology 47 (1998) 342–351.
[9] H. Krim, M. Viberg, Two decades of array signal processing research: the parametric approach, IEEE Signal Processing Magazine 13 (1996) 67–94.
[10] F. Li, R.J. Vaccaro, Unified analysis for DOA estimation algorithms in array signal processing, Signal Processing 25 (1991) 147–169.
[11] A.W. Marshall, I. Olkin, B. Arnold, Inequalities: Theory of Majorization and its Applications, Academic Press, New York, 1979.
[12] A. Paulraj, R. Nabar, D. Gore, Introduction to Space–Time Wireless Communications, Cambridge University Press, New York, 2008.
[13] M. Rubsamen, A.B. Gershman, Direction-of-arrival estimation for nonuniform sensor arrays: from manifold separation to Fourier domain MUSIC methods, IEEE Transactions on Signal Processing 57 (2009) 588–599.
[14] A. Scaglione, P. Stoica, S. Barbarossa, G.B. Giannakis, H. Sampath, Optimal designs for space–time linear precoders and decoders, IEEE Transactions on Signal Processing 50 (2002) 1051–1064.
[15] R. Schmidt, Multiple emitter location and signal parameter estimation, IEEE Transactions on Antennas and Propagation 34 (1986) 276–280.
[16] H. Srinath, V.U. Reddy, Analysis of MUSIC algorithm with sensor gain and phase perturbations, Signal Processing 23 (1991) 245–256.
[17] P. Stoica, A. Nehorai, MUSIC, maximum likelihood, and Cramer–Rao bound, IEEE Transactions on Acoustics, Speech, and Signal Processing 37 (1989) 720–741.
[18] A.L. Swindlehurst, T. Kailath, A performance analysis of subspace-based methods in the presence of model errors. Part I: the MUSIC algorithm, IEEE Transactions on Signal Processing 40 (1992) 1758–1774.
[19] H.L.V. Trees, Detection, Estimation and Modulation Theory. Part IV: Optimum Array Processing, Wiley-Interscience, New York, 2002.
[20] S. Venkatesan, S.H. Simon, R.A. Valenzuela, Capacity of a Gaussian MIMO channel with nonzero mean, in: Proceedings of the IEEE Vehicular Technology Conference, vol. 3, pp. 1767–1771.
[21] E. Visotsky, U. Madhow, Space–time transmit precoding with imperfect feedback, IEEE Transactions on Information Theory 47 (2001) 2632–2639.
[22] M. Vu, A. Paulraj, MIMO wireless linear precoding, IEEE Signal Processing Magazine 24 (2007) 86–105.
[23] M. Vu, A. Paulraj, On the capacity of MIMO wireless channels with dynamic CSIT, IEEE Journal on Selected Areas in Communications 25 (2007) 1269–1283.